THREE-DIMENSIONAL EXTENDED CONTRAST SOURCE INVERSION

Aria Abubakar and Peter M van den Berg
Laboratory of Electromagnetic Research, Delft University of Technology
Mekelweg 4, P.O. Box 5031, 2600 GA Delft, The Netherlands
E-mail: abubakar@its.tudelft.nl

Introduction

A method for determination of the location, shape, and material properties of a 3D object from measurements of the scattered field, when the object is successively illuminated by a number of known incident fields is presented. This work extends the method previously developed for reconstruction of 2D permittivity and conductivity from electromagnetic measurements by a number of line sources surrounding the unknown object (P.M. van den Berg, *et al.*, Inverse Problems, No. 15, 1325-1344, 1999) to the more complicated full-vector 3D inversion. In this paper, we consider inversion from cross-well electrode logging data (static problem), cross-well induction logging data (diffusive problem), and electromagnetic tomography data (electromagnetic problem).

Problem statement

We consider an object, B , of arbitrary bounded cross section. Let D denote the interior of a bounded domain with piecewise smooth discontinuity interfaces. A Cartesian coordinate system is centered in D with spatial points denoted by $\boldsymbol{x} = (x_1, x_2, x_3)$. We assume that the unknown scatterer, B, is contained in the object domain D. The fields are assumed to be varied sinusoidal in time with frequency ω. If the vector $\boldsymbol{E}_j^{\rm inc}$ denotes an incident field with source located at $\boldsymbol{x}_j^{\rm S}$, then for each incident field, the total field $\boldsymbol{E}_j$ in D is given by

$$\boldsymbol{E}_j(\boldsymbol{x}) = \boldsymbol{E}_j^{\rm inc}(\boldsymbol{x}) + \boldsymbol{E}_j^{\rm sct}(\boldsymbol{x})\,. \tag{1}$$

Here, the vector $\boldsymbol{E}$ stands for the electric field vector either for static or electromagnetic problem. It is well known that the total field satisfies the following domain integral equation

$$\boldsymbol{E}_j^{\rm inc}(\boldsymbol{x}) = \boldsymbol{E}_j(\boldsymbol{x}) - [k_{\rm b}^2 + \boldsymbol{\nabla}\boldsymbol{\nabla}\cdot] \int_D G(\boldsymbol{x}-\boldsymbol{x}')\chi(\boldsymbol{x}')\boldsymbol{E}_j(\boldsymbol{x}')\,{\rm d}v(\boldsymbol{x}')\,, \qquad \boldsymbol{x}\in D\,, \tag{2}$$

where

$$k_b^2 = \begin{cases} 0\,, & \\ {\rm i}\omega\mu_0\sigma_b'\,, & \end{cases} \quad \text{and} \quad G(\boldsymbol{x}) = \begin{cases} 1/4\pi|\boldsymbol{x}|\,, & \text{static} \\ \exp({\rm i}k_b|\boldsymbol{x}|)/4\pi|\boldsymbol{x}|\,, & \text{electromagnetic} \end{cases} \tag{3}$$

In Eq. (2), the function χ denotes the contrast of the material properties of the object with respect to its embedding $\sigma_{\rm b}'$, and given by

$$\chi(\boldsymbol{x}) = \frac{\sigma'(\boldsymbol{x}) - \sigma_b'}{\sigma_b'}\,, \quad \text{with} \quad \sigma'(\boldsymbol{x}) = \sigma(\boldsymbol{x}) - {\rm i}\omega\epsilon(\boldsymbol{x})\,, \tag{4}$$

where σ and ϵ are the electrical conductivity and the permittivity distribution. Note that for the static/electrode and diffusive/induction problem, the complex electrical conductivity σ' reduce to a real positive conductivity, σ.
In the inverse scattering problem either the scattered electric potential $V_j^{\rm sct}$ for the static problem or the scattered magnetic field vector $\boldsymbol{H}^{\rm sct}$ for the electromagnetic problem will be measured on data domain S outside D. These integral representations are given by

$$V^{\rm sct}(\boldsymbol{x}) = -\boldsymbol{\nabla}\cdot \int_D G(\boldsymbol{x}-\boldsymbol{x}')\chi(\boldsymbol{x}')\boldsymbol{E}(\boldsymbol{x}')\,{\rm d}v(\boldsymbol{x}')\,, \qquad \boldsymbol{x}\in S\,, \tag{5}$$

and

$$\boldsymbol{H}^{\rm sct}(\boldsymbol{x}) = \sigma_{\rm b}'\boldsymbol{\nabla}\times \int_D G(\boldsymbol{x}-\boldsymbol{x}')\chi(\boldsymbol{x}')\boldsymbol{E}(\boldsymbol{x}')\,{\rm d}v(\boldsymbol{x}')\,, \qquad \boldsymbol{x}\in S\,. \tag{6}$$

In order to discuss our solution of the inverse scattering problem, we write our equations in an operator form and we denote the electric field vector $\boldsymbol{E}_j$ by the symbol u_j and the data quantities either the

scattered magnetic field vector $\boldsymbol{H}_j^{\mathrm{sct}}$ or scalar electric potential field V_j^{sct} by f_j. Then, the data equations in Eqs. (5) and (6) are written symbolically as

$$f_j = G_S \chi u_j \,, \quad \boldsymbol{x} \in S \,, \tag{7}$$

while, the object equations in Eq. (2) written as

$$u_j = u_j^{\mathrm{inc}} + G_D \chi u_j \,, \quad \boldsymbol{x} \in D \,. \tag{8}$$

The inverse scattering problem can now be formulated as follows: finding χ of the object domain D for given f_j at the data domain S, or solving the data equation in Eq. (7) for χ, subject to the additional and necessary condition that χ and u_j satisfy Eq. (8) in D.

Algorithm

A major observation is that the data equation contain both the unknown field and the unknown contrast in the form of a product; it can be written as a single quantity, viz. the contrast source

$$w_j(\boldsymbol{x}) = \chi(\boldsymbol{x})\, u_j(\boldsymbol{x}) \,, \tag{9}$$

which can be considered as an equivalent source that produces the measured scattered field. The data equation in Eq. (7) becomes

$$f_j = G_S w_j \,, \quad \boldsymbol{x} \in S \,, \tag{10}$$

while the object equation in Eq. (8) becomes

$$u_j = u_j^{\mathrm{inc}} + G_D w_j \,, \quad \boldsymbol{x} \in D \,. \tag{11}$$

Substituting Eq. (11) into Eq. (9), we obtain an object equation for the contrast source rather than for the field, viz.,

$$\chi u_j^{\mathrm{inc}} = w_j - \chi G_D w_j \,, \quad \boldsymbol{x} \in D \,. \tag{12}$$

Although the data equation in Eq. (10) is linear in the contrast source, it is a classic ill-posed equation. Therefore, we recasted the problem as an optimization problem in which not only the contrast sources were sought but also the contrast itself to minimize a cost functional. We define the cost functional as follows

$$\mathcal{F}(w_j, \chi) = F(w_j, \chi)\, F_{\mathrm{TV}}(\chi, \delta) = \left[F_S(w_j) + F_D(w_j, \chi)\right] F_{\mathrm{TV}}(\chi, \delta) \,, \tag{13}$$

where

$$F(w_j, \chi) = \frac{\sum_j \|f_j - G_S w_j\|_S^2}{\sum_j \|f_j\|_S^2} + \frac{\sum_j \|\chi u_j^{\mathrm{inc}} - w_j + \chi G_D w_j\|_D^2}{\sum_j \|\chi u_j^{\mathrm{inc}}\|_D^2} \,, \tag{14}$$

and

$$F_{\mathrm{TV}}(\chi, \delta) = \int_D \sqrt{|\boldsymbol{\nabla}\chi(\boldsymbol{x})|^2 + \delta^2}\, \mathrm{d}v(\boldsymbol{x}) \,. \tag{15}$$

The first factor in the cost functional $\mathcal{F}$ contains the errors in the data equation and in the object equation. The second factor in the cost functional $\mathcal{F}$ is the total variation (TV) term. This form of the cost functional in Eq. (13) is chosen such that the optimization process itself determines the weight of the TV-factor. The cost functional in Eq. (13) is based on two things: the objective of minimizing the error in the data equations and object equations and the observation that the TV-factor, when minimized, converges to a constant factor. The structure of the cost functional is such that it will minimize the TV-factor with a large weighting parameter in the beginning of the optimization process, because the value of $F(w_j, \chi)$ is still large, and that it will gradually minimize more and more the error in the data and object equations when the TV-factor has reached a nearly constant value. If noise is present in the data, the data error term will remain at a large value during the optimization and therefore, the weight of the TV-factor will be more significant. Hence, the noise will, at all times, be suppressed in the reconstruction process and we automatically fulfill the need of a larger weight of the TV-factor when the data contains noise. The factor δ^2 in Eq. (15) is introduced for restoring differentiability to the TV-factor. We have chosen the value of δ^2 to be large in the beginning of the optimization and small towards the end. In this way, the optimization will reconstruct the contrast in the first iterations in the normal way, before it will apply the minimization of variation to shape the image further. In particular, we have chosen $\delta^2 = F_{D;n-1}$, in which F_D is the normalized error in the object equations. For a small number of iterations F_D

is large, while it decreases for an increasing number of iterations. The algorithm involves the construction of sequences $\{\chi_n\}$ and $\{w_{j,n}\}$, for $n = 1,\cdots,N$ in the following manner.
Now suppose $w_{j,n-1}$ and χ_{n-1} are known. We update w_j by

$$w_{j,n} = w_{j,n-1} + \alpha^w_{j,n} v_{j,n}\,, \tag{16}$$

where $\alpha^w_{j,n}$ is a constant parameter and the update directions $v_{j,n}$ are functions of position. The update directions are chosen to be the Polak-Ribière conjugate gradient directions, which search for improved directions when a change with respect to the directions of the last iteration occurs and restart the optimization when practically no changes are made in the subsequent gradients. These update directions are obtained as

$$v_{j,0} = 0\,, \qquad v_{j,n} = g^w_{j,n} + \frac{\mathrm{Re}\,\langle g^w_{j,n}, g^w_{j,n} - g^w_{j,n-1}\rangle_D}{\langle g^w_{j,n-1}, g^w_{j,n-1}\rangle_D}\, v_{j,n-1}, \quad n \geq 1\,, \tag{17}$$

where $g^w_{j,n}$ is the gradient (Fréchet derivative) of the cost functional with respect to w_j evaluated at $w_{j,n-1}$ and χ_{n-1}. Explicitly, the gradient for the updating of the contrast source is found in terms of adjoint operators $G^\star_S$ and $G^\star_D$, respectively. With the update directions completely specified, the parameter $\alpha^w_{j,n}$ in Eq. (16) and is found explicitly by minimizing cost functional in Eq. (13). After $w_{j,n}$ has been updated, the field $u_{j,n}$ is known from Eq. (11).
Now suppose χ_{n-1} is known. We update χ by

$$\chi_n = \chi_{n-1} + \alpha^\chi_n d_n\,, \tag{18}$$

where α^χ_n is a constant parameter and the update direction d_n are functions of position. The update directions are again the Polak-Ribière conjugate gradient directions, making the updating scheme consistent with the updating of the contrast sources. These update directions are obtained as

$$d_0 = 0\,, \qquad d_n = g^\chi_n + \frac{\mathrm{Re}\,\langle g^\chi_n, g^\chi_n - g^\chi_{n-1}\rangle_D}{\langle g^\chi_{n-1}, g^\chi_{n-1}\rangle_D}\, d_{n-1}\,, \quad n \geq 1\,, \tag{19}$$

where

$$g^\chi_n = \frac{F_{\mathrm{TV}}\,(\chi_{n-1}, F^{1/2}_{D;\,n-1})\, g^D_n + F(w_{j,n}, \chi_{n-1})\, g^{\mathrm{TV}}_n}{\sum_j |u_{j,n}|^2}\,. \tag{20}$$

The function g^D_n is the gradient of the numerator of F_D in Eq. (13) given by

$$g^D_n = \left(\frac{\sum_j w_{j,n}\overline{u_{j,n}}}{\sum_j |u_{j,n}|^2} - \chi_{n-1}\right) = \frac{\sum_j \left(\chi_{n-1} u_{j,n} - w_{j,n}\right)\overline{u_{j,n}}}{\sum_j |u_{j,n}|^2}\,, \tag{21}$$

and g^{TV}_n is the gradient of the TV-factor F_{TV} in Eq. (13) given by

$$g^{\mathrm{TV}}_n = \frac{1}{2}\boldsymbol{\nabla}\cdot\left[\frac{\boldsymbol{\nabla}\chi_{n-1}}{\sqrt{|\boldsymbol{\nabla}\chi_{n-1}|^2 + \delta^2}}\right]\,. \tag{22}$$

The weighting of the gradients (see Eq. (21)) clearly depends on the errors in the data and object equations F and the TV-factor F_{TV}. The real-valued constant α^χ_n in Eq. (18) is now found to minimize the cost functional in Eq. (13). This minimization can not be calculated analytically and is therefore determined by a numerical line minimization. In this procedure, we take as initial value for α^χ_n the analytical expression obtained by minimizing the cost functional $\mathcal{F}$ in absence of the TV-factor ($F_{\mathrm{TV}} = 1$).
Observe that we cannot start with $w_{j,0} = 0$ and $\chi_0 = 0$, since then the cost functional in Eq. (13) is undefined. Therefore we start with finding the contrast sources that minimize the data error $F_S(w_{j,0})$. Using gradient method, we arrive at

$$w_{j,0} = \frac{\|G^\star_S f_j\|^2_D}{\|G_S G^\star_S f_j\|^2_S} G^\star_S f_j\,. \tag{23}$$

The function $G^\star_S f_j$ is the back propagation of the data from the data domain S into the object domain D. With this initial estimates $w_{j,0}$, the initial field and contrast estimates are obtained by

$$u_{j,0} = u^{\mathrm{inc}}_j + G_D w_{j,0} \qquad \text{and} \qquad \chi_0 = \frac{\sum_j w_{j,0}\overline{u_{j,0}}}{\sum_j |u_{j,0}|^2}\,. \tag{24}$$

Numerical Example

As a test example, we consider the configuration given in Fig. 1 with the contrast function $\chi_1 = 0.6 + 0.2\,\mathrm{i}$ and $\chi_2 = 0.3 + 0.4\,\mathrm{i}$. The test domain D is a cubic with side length 3λ, while the sources are located at plane $x_1 = 3\lambda/2$ and the receivers at $x_1 = -3\lambda/2$. The homogeneous embedding is chosen to be vacuum, therefore $k_\mathrm{b} = 2\pi/\lambda$ ($\sigma'_\mathrm{b} = -\mathrm{i}\omega\epsilon_0$). In the inversion the test domain D is discretized into 14×14×14 subdomains. Thereby amounting to a total of 2744 unknowns complex contrast values. The synthetic data are generated by solving the forward scattering problem numerically with a finer discretization grid (28×28×28 discretization points). In the inversion, we use 25 vertical magnetic dipole sources and 25 multi-components receivers. The reconstruction results from noise-free and data with 10% random white noise are given in Fig. 2. As seen in this figure, the results are quite reasonable despite the large variation of the contrast function and limited amount of data (625 data points). At the conference, we will also present the inversion results from cross-well electrode and induction logging data.

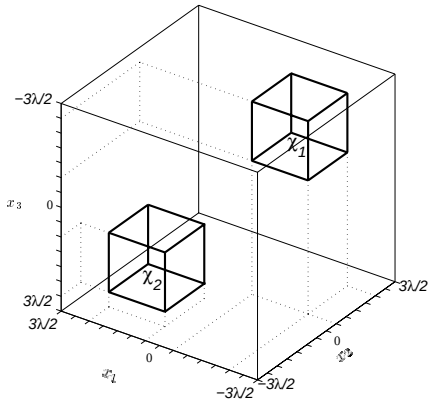

Figure 1: The configuration used to generate the synthetic data with the contrast function $\chi_1 = 0.6 + 0.2\,\mathrm{i}$ and $\chi_2 = 0.3 + 0.4\,\mathrm{i}$. In the inversion, we use 25 sources distributed uniformly at plane $x_1 = 3\lambda/2$ and 25 multi-components receivers at $x_1 = -3\lambda/2$.

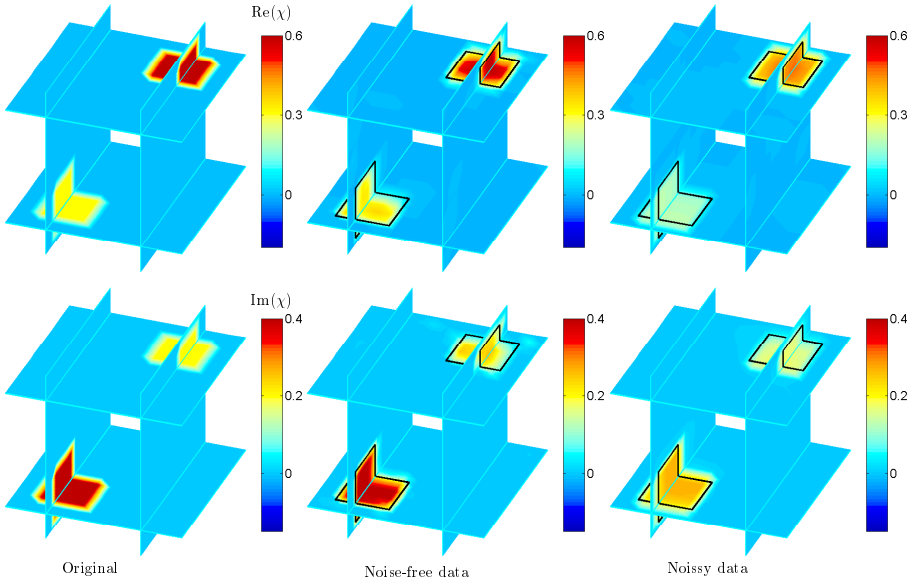

Figure 2: Slices of the 3D real-part of χ distribution (top plots) and slices of the 3D imaginary-part of χ distribution (bottom plots). From left to right are the plots of the original profile, the reconstruction results from noise-free data, and from data with 10% random white noise.